Journal of Fluorescence, Vol. 13, No. 3, May 2003 (© 2003)

Position Dependence of 2-Aminopurine Spectra in Adenosine Pentadeoxynucleotides

Steven P. Davis,[1,2] Masashi Matsumura,[2] Andreia Williams,[1] and Thomas M. Nordlund[2,3]

Received September 17, 2002; revised December 7, 2002; accepted December 10, 2002

The fluorescent probe/base, 2-aminopurine (2AP), has been incorporated into DNA pentamers that otherwise contain only adenine, the base that has been shown to stack strongly with itself and with the adenine mimic, 2AP. The probe base has been placed in each of the five positions in single strands. Optical spectral shifts, energy-transfer efficiencies, and their respective temperature dependencies behave simply as a function of 2AP position: those quantities approximately double when 2AP is placed between two adenines, compared to 2AP at either end of the chain. Transfer efficiencies of 80% (at 5°C) are measured for APAAA and AAPAA, 68% for AAAPA, while PAAAA and AAAAP efficiencies are 52% and 46%, respectively (P = 2AP). The spectroscopic parameters are therefore reliable measures of local DNA conformation that can be interpreted in a straightforward manner in terms of interbase electronic interactions. Interactions of 2AP with nonadenine bases have previously been shown to mostly be much weaker.

KEY WORDS: 2-Aminopurine; DNA; energy transfer; spectral shifts; base stacking; fluorescence.

INTRODUCTION

Measuring meaningful conformations of DNA remains a challenging task, in spite of the advanced capabilities of x-ray (and other) crystallography and multidimensional magnetic resonance techniques. Although important developments have taken place in time-resolved versions of these techniques, procedures based on crystallography and magnetic resonance are not routine or widely available for determining transient structural changes in DNA on arbitrary timescales.[1–14] Optical techniques, on the other hand, have almost arbitrary time resolutions, are nearly universally available in their steady-state versions, but are limited in the molecular detail of information obtained. The dominant modern application of fluorescence probes in DNA has been sequencing—the identification of base types and DNA fragment sizes [15–21]. This identification is made possible by understanding the enzymology of DNA, however, not by understanding the fluorescence spectroscopy of the DNA probes. There is no DNA conformational information obtained from measurements with such fluorescent probes which, as a rule, disturb normal interactions of the DNA with proteins.

Fluorescence of 2-aminopurine inserted at specific DNA sites that interact with enzymes has been used in a number of measurements to demonstrate the time course and mechanism of protein–DNA interactions: protein-induced helix melting, binding constants and kinetic rates, temporal couplings between DNA binding base flipping with the EcoRI DNA methyltransferase, helicase activity, hammerhead ribozyme conformation, proofreading by EcoRI DNA methyltransferase, bacteriophage T4 DNA polymerase, and DNA polymerase I (Klenow

[1]NSF Research Experiences for Undergraduates intern; A.W. from Dept. of Biology, Tuskegee University
[2]Department of Physics, University of Alabama at Birmingham, Birmingham, AL 35294-1170
[3]To whom correspondence should be addressed. nordlund@uab.edu

1053-0509/03/0500-0249/0 © 2003 Plenum Publishing Corporation

fragment). [22–38] These fluorescence measurements have used a small number of parameters to quantitate interactions and structural changes, primarily steady-state fluorescence intensity and steady-state and time-resolved fluorescence and fluorescence anisotropy, sometimes coupled with rapid-mixing techniques. Distinguishing double- from single-stranded DNA, 2AP exposure to water, and local mobility have also been accomplished in large part from time-resolved measurements [39–46]. Measurement of DNA structural changes in the absence of protein have, in addition to the above parameters, used precision fluorescence excitation spectral shifts and the variation of energy-transfer band amplitudes to determine base-stacking interactions, helix melting, base exposure to solvent and base mobility. Electron transfer in DNA [47–51] has been studied using 2AP as an electron acceptor from guanine. [52,53] 2-Aminopurine has also been used as a probe because of its mutagenic activity [54–59], so this useful fluorescence probe must be used carefully.

Careful observation of 2AP fluorescence spectra reveal three general classes of spectroscopic changes: development of energy-transfer bands caused by interaction of 2AP with neighbors, spectral shifts, and intensity and polarization changes. The fluorescence excitation spectrum has proved to be sensitive to structural changes, changing up to about 15 nm (300–315 nm). [43,44,60,61]. New fluorescence excitation bands in the 250–270-nm region have been identified with energy transfer from normal bases, because of the similarity to absorption bands of the normal bases, accompanied by an emission spectrum like that of 2AP [60,62]. The shape and amplitude of these transfer bands depend upon the neighbors of 2AP, with adenine neighbors having order-of-magnitude larger amplitudes, with appreciable transfer over 3–4 adenines, unless interrupted by T,C, or G.

Positions and shifts of (direct) 2AP excitation spectra depend upon the local sequence in which 2AP is inserted [63]. G(2AP)C and C(2AP)G oligonucleotides have relatively blue-shifted excitation spectra compared to the 2AP free base. Hydrogen bonding of the (ground-state) 2AP base with water and interaction with a neighboring guanine seem to be the major causes of the bluer excitation spectra, whereas strong base stacking favors redder spectra and lower fluorescence yield [43,64–66]. The excitation band of 2AP free base is temperature independent; those of (2AP)T, G(2AP)C, C(2AP)G, and TT(2AP)TT shift about 0.35 nm/50°C (shift to the blue as temperature rises); A(2AP)T shifts about 0.9 nm/50°C rise, just rising to the position of the free base at high temperature. On the other hand, the decrease of fluorescence yield with increasing temperature is smallest for A(2AP)T, even compared to the free base. The dominant interbase interaction when A neighbors 2AP appears to be temperature-dependent stacking with accompanying energy transfer, while in G- and C-containing trinucleotides a temperature-independent interaction keeps the 2AP excitation spectrum blue-shifted. Evans has proposed an intrastrand H bond, on the basis of the unusual short-wavelength excitation spectrum of G(2AP)C and preliminary molecular dynamics simulations, which show the O6 of guanine can stabilize itself within hydrogen-bonding distance of the NH_2 of 2AP [67]. The effect of double strand formation on spectral shift in these short oligomers appears to be small compared to stacking interaction effects [63]. No evidence for fluorescent excited-state complexes (exciplexes) of 2AP with neighboring bases (usually accompanied by a large red-shifted emission) has so far been described [68,69].

Jean and Hall have recently used time-dependent density functional theory to describe the excited and ground states of dimers of 2AP with the four normal bases, oriented in B-form orientations, and, in the case of 2AP-T, also in the A-form [70]. They find that 2AP fluorescence is quenched statically in 2AP/purine dimers by significant ground-state mixing of the 2AP and (weakly fluorescent) A or G orbitals, while 2AP/pyrimidine dimers are quenched dynamically by rapid relaxation of the initial excited state to a lower "dark" excited state. These results are in general agreement with the observations [62] (and this work) that efficient energy transfer occurs in DNA oligomers with As on either or both sides of 2AP, and that the efficiency is reduced as temperature increases, breaking up the adenine-2AP stacks and eliminating the ground-state orbital mixing. However, a more comprehensive treatment of this transfer phenomenon must be done. Likewise, the stacking-induced orbital mixing is consistent with the relative stronger temperature dependence of fluorescence excitation spectrum of 2AP with neighboring A [63] (and this work), with the spectrum of the oligomer shifting to that of the 2AP free base at high temperature, where the stacking is eliminated. The fact that Jean and Hall find that the 2AP/T dimer states change in the A-DNA conformation, however, indicates that the interpretation of spectra needs careful consideration of the conformation or conformations involved. Stated in a positive sense, measurement of oligomer spectra and comparison with theoretical calculations allows direct optical spectral determination of oligomer local conformation, a goal of ours and other workers.

The present study examines in more detail the behavior of the optical spectra of single-stranded PAAAA, APAAA, AAPAA, AAAPA, AAAAP oligomers (P = 2AP = 2-aminopurine), to determine the position dependence of fluorescence spectra in adenine oligodeoxynucleotides.

Addition of excess TTTTT complement to these strands did not produce definitive evidence for double-strand formation, though spectral shifts and energy transfer bands could still be observed. We concentrate again, in this work, on *straightforward* methodologies that can be used in any laboratory equipped with a good fluorometer, performing simple but precision data analysis on Excel spreadsheets or virtually any modern, commercial graphing program. The results are quite simple: spectra of oligomers with 2AP at the end are substantially the same; spectra of oligomers with an interior 2AP are similar to each other.

MATERIALS AND METHODS

2-Aminopurine free base was used as purchased from Sigma Chemical Co. (St. Louis, MO, USA), while 2AP-containing oligodeoxynucleotides were obtained from Macromolecular Resources (Colorado State University, Ft. Collins, CO, USA). The latter were provided purified by reverse-phase liquid chromatography and characterized by MALDI mass spectrometry. Our own (unpublished) NMR measurements of oligomers obtained for previous work show very low levels of impurities, allowing collection of high-quality proton 2D NMR spectra. Samples were dissolved in 20 m*M* pH 7.3 Tris-Cl buffer containing 100 m*M* KCl and 0.1 m*M* EDTA. Single-stranded concentrations were approximately 15–20 μ*M* for fluorescence measurements. Single-strand concentrations can be found from the 260-nm extinction coefficients of Puglisi and Tinoco [71], with extinction coefficients of 2AP-containing strands from Xu and Nordlund [62]. The needed dimer extinction coefficients are $\varepsilon_{260}(\text{AP}) \approx \varepsilon_{260}(\text{PA}) \approx 8.13 \times 10^3\ M^{-1}\cdot\text{cm}^{-1}$. The resulting strand extinction coefficients are $\varepsilon_{260}(\text{PAAAA}) \approx \varepsilon_{260}(\text{AAAAP}) \approx 52.1 \times 10^3\ M^{-1}\cdot\text{cm}^{-1}$; $\varepsilon_{260}(\text{APAAA}) \approx \varepsilon_{260}(\text{AAPAA}) \approx \varepsilon_{260}(\text{AAPAA}) \approx \varepsilon_{260}(\text{AAAPA}) \approx 54.6 \times 10^3\ M^{-1}\cdot\text{cm}^{-1}$; $\varepsilon_{260}(\text{TTTTT}) \approx 42.8 \times 10^3\ M^{-1}\cdot\text{cm}^{-1}$. The concentration of a strand containing a single 2AP can also be quickly approximated from the 305-nm absorbance of 2AP, using $\varepsilon_{305} \approx 7.2 \times 10^3\ M^{-1}\cdot\text{cm}^{-1}$.

Absorption spectra and melting determinations were measured with a Response II spectrophotometer (Gilford/Corning, Walpole, MA, USA) with built-in, computer-controlled thermoelectric temperature controller, using 1.0-nm bandwidth and 1.0-cm path length cuvets. Spectra were transferred to a PC and imported into an Excel spreadsheet for further analysis and plotting. Fluorescence spectra were measured with a Fluoromax 2 fluorometer (SPEX/ISA, Inc., Edison, NJ, USA), in 0.3- × 0.3-cm cuvets, typically using 3.0-nm excitation and emission bandwidths and recording in 2-nm steps. Temperature was controlled by a Neslab RTE-5DD circulator (Newington, NH, USA). Sample versus bath temperature calibration was done by placing a thermistor probe (Omega, Stamford, CT, USA) in a water-filled cuvet and measuring both temperatures. Spectra were recorded in their raw form, with spectrometer correction files (reference beam intensity) stored separately for later correction, along with factors correcting for sample absorbance.

DATA ANALYSIS

Concentrations of these short oligomers (Table I) were kept high enough (at least 10^{-5} M) so that single-strand results can later be compared to duplex DNA measurements. The resulting absorbance in the 250–270 nm region produces moderate reduction of the excitation beam through the 0.30-cm excitation beam path, thus reducing the relative fluorescence excited by 260-nm light

Table I. Optical Parameters and Oligomer Conditions

Oligomer	ε ($M^{-1}\cdot\text{cm}^{-1}$)	Concentration used (μ*M*)	β*	Δλ/50°C (nm/50°C)†	Energy transfer efficiency (% at 5°C, λ_{ex} = 254 nm)
PAAAA	52,100	21	21.4	1.20	52
APAAA	54,600	22	20.8	3.03	80
AAPAA	54,600	16	20.4	2.62	80
AAAPA	54,600	16	20.6	2.29	68
AAAAP	52,100	19	22.0	1.36	46
TTTTT	42,800	NA	NA	NA	NA

*$\Delta\lambda = \beta\Delta I$. Units: nm/unit fractional, normalized intensity difference. Errors approx ±0.3. β is sensitive to the shape of the spectrum, but here plays no role other than to assist in precise determination of spectral shift with temperature.
†Shift of direct 2-aminopurine excitation band with temperature.

compared to 310–320-nm light, where the sample absorbance is an order of magnitude less. However, in quantifying the shift of the 310-nm band, high absorption is not a problem and we find it more prudent to analyze raw spectra, rather than corrected spectra, which contain additional noise resulting from the correction process. We employ a difference method, previously described [63], to quantify fluorescence excitation spectral shifts and shape changes as a function of temperature. A reference spectrum, the high-temperature limiting spectrum, is subtracted from the spectrum at each temperature, T, after all spectra are normalized at the (direct) excitation peak of 2AP in the DNA being measured.

Fluorescence Spectral Shifts

The shift found by this method is relative to the reference spectrum, which, in the high temperature limit, would be expected to approximate that of the 2AP free base. If the peak or centroid of the reference spectrum is obtained, the relative shifts can be converted to absolute shifts. If spectral changes are small and the change is a pure shift, $\Delta\lambda = \beta * \Delta I$, where β is the slope of the wavelength shift vs maximum difference spectral amplitude ΔI. Values of β are tabulated in Table I. Values of β found previously for deoxyoligomers ranged from 27.2 to 30.3 nm per unit difference spectral amplitude. [44] The lower values in this work reflect the present direct treatment of spectra versus wavelength, rather than versus wavenumber and the different spectral shapes resulting from analysis of uncorrected spectra.

Formation of Double-Stranded DNA?

Short oligomers, especially those consisting entirely of adenine, do not readily form double helices, because of the small number of potential base pairs and the lesser stability of A-T hydrogen bonds compared to those of G-C. An estimate of the T_m of 2AP-containing DNA can be made by assuming that 2AP neither forms a base pair nor inhibits adjacent bases from pairing, for example APAAA/TTTTT is equivalent to AAAA/TTTT. Melting temperatures for a AAAA/TTTT were 8°C, 12°C, and 19°C for TTTTT concentrations of 50, 100, and 300 μM, respectively, using the Pasteur Institute web site calculator (bioweb.pasteur.fr/seqanal/interfaces/melting.html), with Breslauer theory and Santa Lucia salt correction [72]. (Calculations using some other algorithms gave significantly lower T_m values.) With a concentration of 300 μM TTTTT, fluorescence measurements extending down to the 250–280 nm region are simple to perform but more difficult to correct because of the large absorbance of excess TTTTT. We clearly observe energy transfer, but the apparent amplitude of the energy transfer peak is somewhat reduced because of high absorbance of the sample at 260 nm. The temperature-dependent absorption spectra of these A-T oligomers do not show clear evidence for ds formation. The strand shortness ensures cooperativity is low; furthermore, the absorption changes in the 240–280 nm region are neither simple hypochromism nor spectral shifts, preventing quantitative analysis of the fraction of double-strand formation. The spectral changes of the 2AP-containing strands and the TTTTT complement individually show changes comparable to those in the double strand. The T_m estimates above suggest double strands are formed, at least below about 10°C, but the spectroscopic evidence is unclear. We therefore postpone double strand studies to oligomers with more clearcut melting curves.

Energy Transfer

After ensuring that the emission spectrum is characteristic of 2AP at all excitation wavelengths, energy transfer can be demonstrated if an excitation band characteristic of a donor molecule is observed. In the present case, the development of an excitation band in the 250–270 nm region, where the isolated 2AP free base has an absorption minimum, shows energy transfer from adenine to 2-aminopurine. The transfer efficiency η_t from donor to acceptor can be calculated as [62]

$$\eta_t(\lambda_{ex}) = \frac{A_a(\lambda_{ex})}{A_d(\lambda_{ex})}\left[\frac{F(\lambda_{ex})}{F_a(\lambda_{ex})} - 1\right] \qquad (1)$$

where $F(\lambda_{cx})$ is the fluorescence intensity of the oligomer, excited at wavelength λ_{ex}, $F_a(\lambda_{ex})$ is the fluorescence intensity of directly excited energy acceptor (2AP); $A_a(\lambda_{ex})$ is the absorbance of energy acceptor (2AP); and $A_d(\lambda_{ex})$ is the absorbance of energy donors (normal bases in DNA). In this equation, $A_a(\lambda_{ex})$ and $F_a(\lambda_{ex})$ must be measured from 2AP deoxynucleoside (dns), multiplying the latter intensity by the ratio ϕ_0(2AP-dns)/ ϕ_0(2AP in oligo) to account for the yield difference between the two samples. An approximation that does not require separate measurement of $F_a(\lambda_{ex})$, but that assumes there is no absorption spectral overlap between donor and acceptor [73], is

$$\eta_t(\lambda_d) = \frac{F(\lambda_d)\left(1 - 10^{-A(\lambda_a)}\right)}{F(\lambda_a)\left(1 - 10^{-A(\lambda_d)}\right)} \qquad (2)$$

where λ_d is a wavelength where only the donor (adenine) absorbs, λ_a is the excitation wavelength maximum of the

acceptor (2AP), F(λ) is the measured fluorescence when excited at λ, and it is assumed the donor does not absorb at λ_a. In oligonucleotides that contain the acceptor 2AP, the absorbance of the donors (normal bases) overlaps the absorbance of acceptor to a minor extent. The absorbance of the acceptor $A_a(\lambda_a)$ can be directly read from $A(\lambda_{ex})$ of the oligomer. An energy-transfer spectrum can be plotted by calculating η_t at all wavelengths where the 2AP absorption does not appreciably overlap that of the normal bases, that is from about 250 to 280 nm. Where 2AP absorption dominates that of the normal bases, naive use of Eq.(2) (donor and acceptor both 2AP) will give, in fact, a measure of the excitation wavelength dependence of the 2AP quantum yield. Previously, only moderate excitation wavelength dependence was found for the efficiency [61].

In contrast to the spectral shift analysis, energy-transfer determinations must use corrected spectra, because they rely directly on the ratio F_{260}/F_{310}. We correct ss spectra for excitation beam attenuation using the method described in Nordlund *et al.* [73], by multiplying the measured fluorescence intensity at each excitation wavelength λ_{ex} by the approximate factor $CF=\frac{2.303*A(\lambda_{ex})}{1-10^{-A(\lambda_{ex})}}$

An even larger effect, however, is the correction for spectrometer optics (reference beam channel plus software corrections coming from spectral standards, reflecting excitation beam intensity versus wavelength, diffraction grating, and detector and other component wavelength dependence). After all correction factors are included, our fluorometer sensitivity is roughly 3.8 (3.1) times lower at 266 (270) nm than at 310 nm. Calculated transfer efficiency is directly proportional to this relative sensitivity factor; thus the reliability of the correction is critical. We therefore measured the correction factor two independent ways: (i) from the standard, front-face excitation spectrum of concentrated rhodamine B in ethylene glycol [74] and (ii) from measurement of the low-concentration excitation spectrum of rhodamine B and the corresponding absorption spectrum. In the latter case, because the quantum yield is independent of excitation wavelength, calculation of the quantity $(1–10^{-A(\lambda)})/F(\lambda)$ at each wavelength provides a relative correction factor at each excitation wavelength. These two ways of determining the fluorometer excitation-wavelength-dependent correction factors differed from each other 1–8% in the region of interest. The largest differences are observed in wavelength regions on the steeply sloping sides of the rhodamine excitation peaks, where relative wavelength calibration errors between the absorption and fluorescence spectrometers cause larger deviations. We used the standard front-face correction file (method I) for calculation of transfer efficiencies.

RESULTS

Absorption Spectra

The temperature-dependent absorption spectrum of PAAAA and AAPAA, shown in Fig. 1, are typical of the ss pentamers containing one 2AP, with a peak corresponding to adenine near 257 nm and one to 2AP at 305–312 nm. The peak for 2AP in the latter oligonucleotide is farther to the red, because of its greater stacking with adjacent bases and less exposure to water and potential H bonds, consistent with previous observations.[43,44,60,62,63] A plot of A(260 nm) versus T for PAAAA shows a roughly linear absorption increase of about 9.0% per 50°C temperature rise; that for AAPAA rises 7.9% per 50°C. A shift of the 2AP peak to shorter wavelength as temperature increases is also observed, as has been pointed out previously.

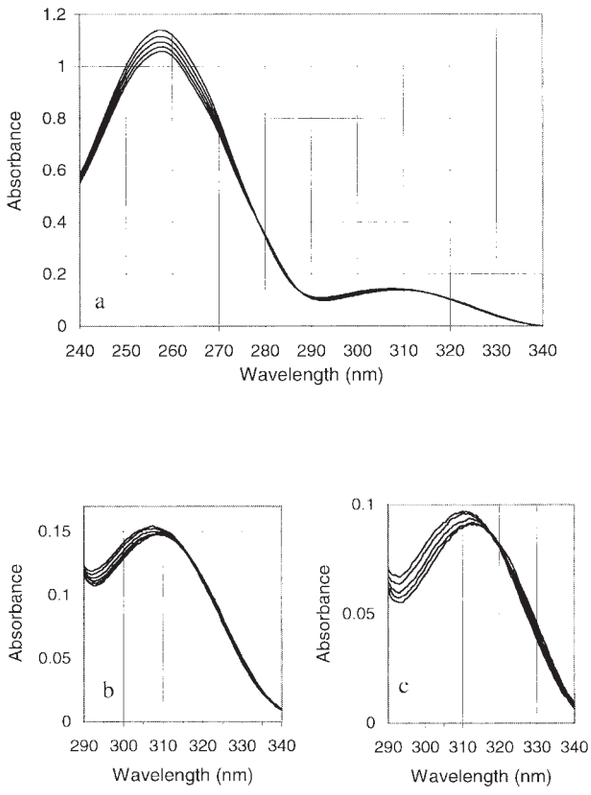

Fig. 1. Absorption spectra versus temperature. (a) and (b), PAAAA; (c), AAPAA. Temperature range 5–45°C, bottom to top, spaced equally in temperature. Absorption experiments used 1-cm path length cuvets, fluorescence measurements, a 3-mm cuvet.

Fluorescence Spectra

The fluorescence excitation spectrum of the PAAAA oligomer has a simple temperature dependence (Fig. 2). The spectra of the AAAAP oligomer (not shown) are almost identical to those of PAAAA, showing that the 5′ versus 3′ end location has little spectral effect. The spectrum of the directly excited base in the 290–330 nm region shifts to shorter wavelength and reduces its intensity as temperature increases. Simultaneously, an energy-transfer band in the 250–280 nm region (where adenine absorbs) decreases in amplitude. Both of these effects are clearly shown in the difference spectrum in Fig. 2b. The 290–340 nm spectral derivative-like shape is characteristic of an almost pure spectral shift. This difference spectrum is calculated by first normalizing the spectra at the peak of the 310-nm band; thus the decrease of the intrinsic 2AP fluorescence yield is removed. If the far-UV band simply scaled in amplitude with the 310-nm band, no difference peak would be evident at 260–270 nm. Obviously, the latter band has a much stronger temperature dependence. As will be shown later, application of spectral correction to this region shows the 260-nm amplitude is even larger than is apparent in Fig. 2.

The AAAPA oligomer shows the same spectral changes with temperature as PAAAA and AAAAP, but all effects are about a factor of two times larger (Fig. 3). Spectra of APAAA and AAPAA (not shown) are almost identical to those of AAAPA, showing that the interior-base excitation spectrum and its temperature dependence depend only weakly on position in the oligomer, as long as the location is not at the end.

The temperature dependences of the 310-nm excitation bands for all five oligomers are shown in Fig. 4. The shift of all spectra is to shorter wavelength as temperature increases and is close to linearly dependent on temperature in the 5–50°C range. The slopes of the lines for PAAAA and AAAAP, 1.20 and 1.36 nm/50°C, are very close to a factor two smaller than those of APAAA, AAPAA, and AAAPA, which are 3.03, 2.62, and 2.29 nm/50°C, respectively (Table I). The gradual decrease of the temperature dependence as the interior 2AP base is moved toward the 3′ end is apparently real, however, as the estimated errors in slope are about 3%.

An example of a fully corrected fluorescence excitation spectrum (Fig. 5) shows two major facts: (i) the

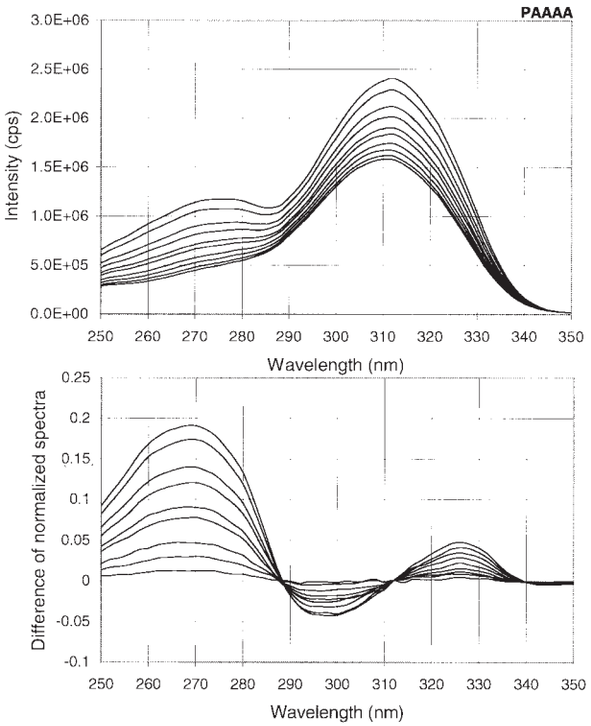

Fig. 2. Fluorescence excitation spectra versus temperature, PAAAA. (a) Raw spectra; (b) difference of normalized spectra. The reference spectrum is that measured at 50°C. The spectra of AAAAP are almost identical. Temperature range 5–50°C, top to bottom, spaced equally in temperature.

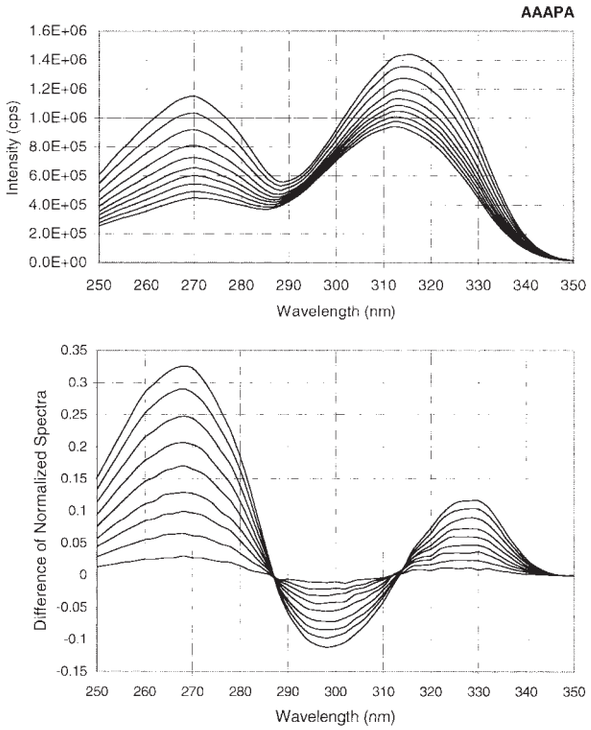

Fig. 3. Fluorescence excitation spectra versus temperature, AAAPA. (a) Raw spectra; (b) difference of normalized spectra. The reference spectrum is that measured at 50°C. The spectra of APAAA and AAPAA are almost identical to that of AAAPAs. Temperature range 5–50°C, top to bottom, spaced equally in temperature.

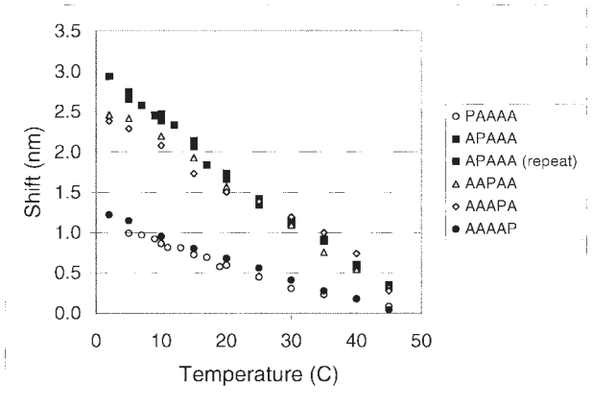

Fig. 4. Shift of the ~310-nm, 2AP direct excitation fluorescence band versus temperature. The shift and its temperature dependence is close to a factor two larger when 2AP has adenine on both sides, as compared to one side: PAAAA, 1.20 nm/50°C; AAAAP, 1.36 nm/50°C; APAAA, 3.03 nm/50°C; AAPAA, 2.62 nm/50°C; AAAPA, 2.29 nm/50°C; errors ±3%.

amplitude of the 260-nm band is much higher than in the raw spectrum, and (ii) both spectral positions are farther to the UV. Although this correction has little effect on the spectral-shift calculations, which are all relative to a reference spectrum, it does affect the absolute spectral positions and (especially) the absolute heights of the bands. These corrected spectra are similar to those in Xu *et al*. (Fig. 5) [62] on a AAAAPAAAAA DNA decamer. The latter spectra show somewhat more structure in the 240–270 nm region, but we do not presently attach significance to these differences, because they were

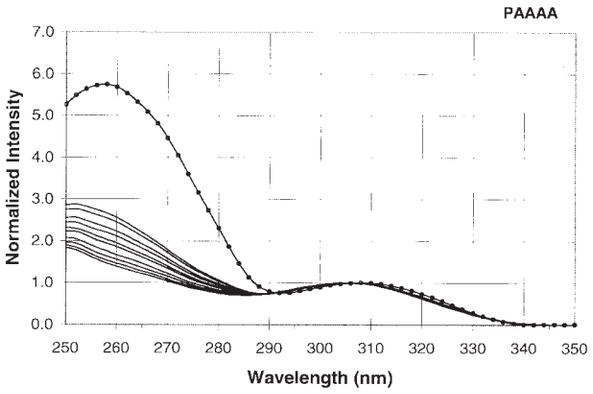

Fig. 5. Corrected fluorescence excitation spectra of PAAAA from 5 to 50°C (solid lines, top to bottom). Raw recorded fluorescence intensities (cps) were corrected for high absorption and for spectrometer factors (excitation intensity, gratings, and other optics, etc.) and then normalized at the ~310–nm peak. If transfer were 100% efficient, the excitation spectra would coincide with the normalized absorption probability spectrum (line plus points).

recorded on a different fluorometer in the most difficult spectral region and because the particular Xu *et al*. spectrum shown is not corrected for sample absorption. (Their later calculations corrected for this.)

Energy transfer

The percentage of energy transfer in the low-absorbance limit Eq. (2) can be seen to be 100% if the ratio of the 260–310 nm excitation peaks is the same as that ratio of a absorption probability spectrum calculated as $(1–10^{-A(\lambda)})$.

PAAAA and AAAAP

A quick comparison of the peak ratios (255–260 nm to 305 nm) for the absorption probability spectrum $(1–10^{-A(\lambda)})$ and excitation spectra of PAAAA in Fig. 5 gives an estimate of η_t(260 nm) ~50% at 5°C; a more exact calculation gives 52 ± 5%, where the uncertainty is obtained from estimates of the spectral correction uncertainties and of nonzero overlaps between absorption bands of donor and acceptor at 260 nm and 310 nm (Table I). The transfer efficiency in AAAAP is 46%, somewhat lower that in PAAAA.

APAAA, AAPAA, and AAAPA

The fluorescence excitation spectra of these oligomers are similar, indicating that transfer is similar in all. However, transfer in these oligomers, 80%, 80%, and 68%, respectively, is significantly higher than in PAAAA and AAAAP, 51% and 46%. This can be explained by the number of As directly adjacent to the energy acceptor, 2AP. In APAAA, AAPAA, and AAAPA, two As are adjacent; in PAAAA and AAAAP, only one is. This is consistent with decrease of A → 2AP transfer with increasing distance of donor to acceptor base, reported in Xu *et al*. [62]. These efficiencies can be compared to the value of 46 ± 5% of Xu *et al*. [62], for transfer in the AAAAPAAAAA oligomer at 5°C. However, in the longer oligomer, the efficiency may be expected to be lower than that in the pentamers, because the average distance of As from 2AP is greater.[4] If bases removed from P further than 2 do not transfer at all

[4]What we call the "total" transfer efficiency can also be thought of as the "average" transfer efficiency from all bases that absorb at the donor wavelength, 260 nm. We would expect A bases farther from 2AP to transfer energy less efficiently than those closer; thus a longer oligomer would, a priori, be expected to have a lower "total" or "average" transfer efficiency.

(assume symmetry in direction), then the efficiency of AAAAPAAAAA compared to AAPAA would be η(AAAAPAAAAA) = (4/9)η(AAPAA) = (4/9)(80%) = 36%; if further than 3, then η(AAAAPAAAAA) = (6/9)(80%) = 53%. However, in view of the large correction on η imposed by fluorometer correction factors and the two different fluorometers used, as well as the mild sequence dependence of h (e.g., AAPAA and APAAA vs. AAAPA), the agreement should be considered tentative.

Wavelength Dependence of η

Plots of the ratio of the corrected, normalized excitation spectra to the excitation probability spectrum in Fig. 5 produce an energy transfer spectrum (Fig. 6). The region of validity of these spectra is about 250–280 nm, or until the 2AP direct excitation probability is appreciable. These spectra suggest that transfer is somewhat more efficient at shorter wavelengths, especially for the PAAAA and AAAAP. In the region from about 295 to 325 nm, where 2AP absorption dominates, this calculated plot assumes 2AP is both donor and acceptor. The value gives the photon emission probability divided by the absorption probability; thus the 300 to 330 nm really shows the excit-ation wavelength dependence of the fluorescence quantum yield, normalized to 1 at the peak of the 2AP excitation excitation peak in the oligomer. The data suggest a wavelength dependence of the quantum yield, with somewhat higher values at shorter wavelengths. The erratic behavior beyond 330 nm may be due to the small excitation probability and the likelihood that the wavelength dependence of the two detection systems, absorption and fluorescence, are not, in fact, identical.

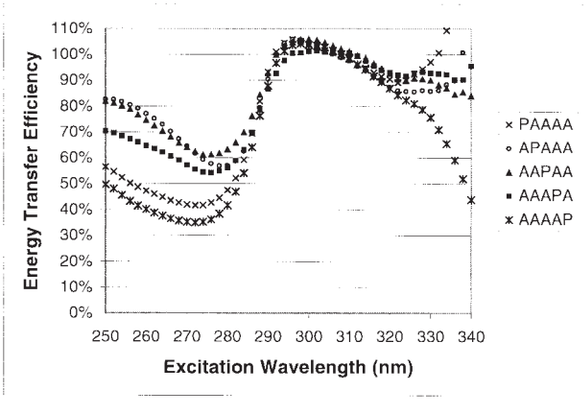

Fig. 6. Energy transfer spectra of single strands at 5°C. Above 280 nm, direct 2AP excitation distorts the calculated transfer. The apparent efficiency goes above 100% near 300 nm because the curve in this region of direct 2AP excitation actually reflects the relative quantum yield, which was normalized to 1 at the 2AP peak in the 305–312 nm region.

DISCUSSION

The position dependence of fluorescence properties of 2AP in adenine-containing DNA pentadeoxynucleotides is quite simple, to a first approximation: the primary properties depend on whether 2AP has one or two adenine neighbors. The shift of the excitation spectrum and its temperature dependence in single strands is twice as much in APAAA, AAPAA, and AAAPA as in PAAAA and AAAAP; the energy-transfer efficiency in the former oligomers is roughly 1.5 times that of the latter. These two spectral properties provide convenient spectral "handles" on the environment of the 2AP. The shift is small, but can easily be measured using difference techniques, even in the presence of a large excess of nonlabeled DNA. Energy transfer provides a 2AP fluorescence excitation band whose temperature dependence is much greater than that of the direct excitation band, a band that is unique to 2AP neighbored by adenines and is sensitive to adenine stacking over distances of several bases. (Transfer from C, T, and G to 2AP is an order of magnitude less efficient [62], though we have recently observed efficient transfer from G to 2AP, but only when 2AP is at the 3′ end of a G strand: GGGGP [75].) This transfer band could be used, for instance, for real-time monitoring of the cleavage of an adenine base near a 2AP base.

Spectral characteristics of 2AP should be described to first order in terms of the number of stacking adenine neighbors, not in terms of end-of-strand effects. The fact that stacking-induced shifts and energy transfer efficiencies are about 1.5–2 times as high for interior 2APs seems to imply that end effects are negligible for most of the measurements. True "end effects" would be more relevant when investigating structural changes involved in duplex formation, which, as we have shown, requires measurements below 0°C for mostly adenine pentamers. Such low-temperature measurements entail use of special solvents and are beyond the scope of the present work. To a second approximation, it appears that energy transfer tends toward lower efficiency near the 3′ end of the strand.

We have found that analysis of the 240–280 nm absorbance of 2AP-containing oligonucleotides with large excesses of the nonlabeled complement can be carried out by carefully subtracting the temperature-dependent absorbance of the excess (unbound) complement. This analysis will be presented in a companion paper (Davis *et al.*, to be published) for the case of guanine strands with cytosine complements (e.g., GGGGP/CCCCT),

where the case of ds formation is clearer. What we find in these cases is that standard A_{260} versus T still does not always reflect duplex formation; the 240–280 nm spectral changes with temperature can be more complex than simple hypochromism. Spectral regions can be found where absorbance increases or decreases with T, with various functional dependencies, or even remains ~constant. Though these difficulties decrease in long nucleic acids, where the differing spectral changes of the four bases remarkably average to produce an approximate hypochromic effect at 260 nm, it is important to check in each case that A_{260} does, in fact, accurately measure helix formation and melting.

Recent theoretical studies on 2AP dimers with each of the four other bases are important to consider in the interpretation of our spectral shift results. Jean and Hall [70] have used time-dependent density functional theory to calculate the ground and excited states of such dimers and have concluded that purine and pyrimidine neighbors to 2AP interact quite differently with 2AP. Placing the two bases in B-DNA orientations, they found that guanine and adenine stack strongly with 2AP, causing ground state mixing of the A (or G) and 2AP orbitals. Such ground state mixing has several effects. Jean and Hall focus on the perturbation of absorption (and fluorescence excitation) spectra and the reduction of fluorescence yield due to this mixing. Though their calculations are not designed to study transfer, ground-state mixing also implies that energy absorbed by A (or G) is, in fact, delocalized and can populate the 2AP excited state, from which fluorescence occurs. Such ground-state mixing does not occur in dimers of 2AP with T or C, where fluorescence quenching results from relaxation to a "dark" (non-emitting) excited state, which is not optically accessible directly from the ground state. Our measurements support these theoretical results for A, C, and T. Our previous measurements show that the excitation spectrum of 2AP with C and/or T neighbors is less perturbed from 2AP free-base spectra and is less sensitive to temperature than are A-neighbored 2AP [62,63]. The spectral predictions for G-2AP dimers are not in accord with our (previous) fluorescence measurements, however. We will deal with this in detail in future work, but it appears likely that the theoretical assumption of B-conformation is not correct, at least for short oligomers, possibly because of intrastrand interaction of the 2AP amino group with the guanine O6 [62,67].

We and others have previously considered Förster ($\eta \propto 1/r^6$ very weak coupling) energy transfer in DNA [62, 76–80]. Such theory should not apply, in principle, because of the proximity and orbital overlap of adjacent bases; furthermore, the distance dependence of the Förster theory did not match the data analysis of Xu *et al*. [61,62]. (This latter calculation did not, however, take into account the variation of the dipole–dipole orientation factor present in Förster theory.) Furthermore, spectral shifts, as observed in this work, as well as the Jean and Hall calculations, imply a strong interaction between donor (2AP neighbor) and acceptor (2AP), inconsistent with Förster $1/r^6$ theory. The observation that emission from these pentamers, excited in the 260-nm region, has the characteristic spectrum of 2AP, while calculations show ground-state mixing of A and 2AP, are not necessarily inconsistent, but do need a proper resolution, In view of the recent success of theoretical calculations on 2AP-containing dinucleotides, it would appear timely to apply a more appropriate transfer theory to AP and PA dinucleotides, as well as APA trinucleotides.

CONCLUSIONS

A primary design purpose of 2AP is as a base that can act as a probe of nucleic acid structure and interactions with proteins and its environment, especially during biologic activity. As with any probe, careless (or planned) use of the base can result in unintended (or intended) perturbations of structure. How can our present results be used to help optically probe DNA activity? We have characterized three spectral measures of DNA containing 2AP with adenine neighbors: fluorescence excitation spectral shifts, a ~260-nm A→2AP energy transfer band, and fluorescence intensity changes. All these measures depend primarily on A-2AP stacking interactions. The weak dependence of these measures on interior position of 2AP within the adenine strand is a great simplification, as one can then focus on probing, for example, stacking interactions without having to adjust the analysis for each separate probe position. The simple, factor-of-about-two change in temperature sensitivity of spectral position and energy-transfer efficiency when 2AP goes from having two to one adenine neighbor, as well as the greater sensitivity of A-2AP stacks compared to T-2AP, C-2AP, or G-2AP, are likewise advantageous when probing, for example, cleavage or unstacking of a particular adenine at any point in a helix. Fluorescence intensity, as well as polarization, can also be used as probes of cleavage and unstacking, as shown by a number of studies.

Finally, much has recently been made of the possibility that DNA can acts as a "molecular wire"—an efficient conductor of charge—with conclusions ranging from insulator to superconductor. Whereas supporting electrical measurements on DNA are difficult, excitation energy transfer measurements of the sort presented here

are straightforward and show that transfer efficiencies approach 100% in short, adenine-dominated oligomers near 0°C. Use of carefully designed DNA as a "molecular fiber optic" is therefore a possibility. The next step in these studies is to introduce excitation selectively at one end and observe transfer to a 2AP at the other end of the DNA strand.

ACKNOWLEDGMENTS

This work is supported in part by grants from the National Science Foundation grants MCB-9723278 and Research Experiences for Undergraduates grant DMR 9619405 (support of AW), and NIH grant CA94327.

REFERENCES

1. R. D. Frankel and J. M. Forsyth (1985) *Biophys*. J. **47**(3), 387–393.
2. Y. Amemiya, K. Wakabayashi, and H. Tanaka (1985) *Tanpakushitsu Kakusan Koso - Protein, Nucleic Acid, Enzyme* (28), 268–273.
3. W. A. Caffrey, R. L. Magin, B. Hummel, and J. Zhang (1990) *Biophys*. J. **58**(1), 21–30.
4. A. P. Mencke and M. Caffrey (1991) *Biochemistry* **30**(9), 2453–2463.
5. A. Cheng, B. Hummel, A. Mencke, and M. Caffrey (1994) *Biophys. J*. **67**(1), 293–303.
6. G. Stubbs (1999) *Curr. Opin. Struct. Biol*. **9**(5), 615–619.
7. B. Perman, S. Anderson, M. Schmidt, and K. Moffat (2000) *Cell. Mol. Biol*. **46**(5), 895–913.
8. J. Balbach, V. Forge, N. A. van Nuland, S. L. Winder, P. J. Hore, and C. M. Dobson (1995) *Nature Struct. Biol*. **2**(10), 865–870.
9. H. Ernst, D. Freude, T. Mildner, and I. Wolf (1996) *Solid State Nucl. Mag. Reson*. **6**(2), 147–156.
10. P. Gouet, H. M. Jouve, P. A. Williams, I. Andersson, P. Andreoletti, L. Nussaume, and J. Hajdu (1996) *Nature Struct. Biol*. **3**(11), 951–956.
11. B. Perman, V. Srajer, Z. Ren, T. Teng, C. Pradervand, T. Ursby, D. Bourgeois, F. Schotte, M. Wulff, R. Kort, K. Hellingwerf, and K. Moffat (1998) *Science* **279**(5358), 1946–1950.
12. A. K. Bhuyan and J. B. Udgaonkar (1998) *Proteins* **32**(2), 241–247.
13. R. Subramanian, W. P. Kelley, P. D. Floyd, Z. J. Tan, A. G. Webb, and J. V. Sweedler (1999) *Analyt. Chem*. **71**(23), 5335–5339.
14. H. Kato (2001) *Tanpakushitsu Kakusan Koso Protein, Nucleic Acid, Enzyme* **46**(11 Suppl), 1446–1455.
15. R. A. Keller, L. A. Bottomly, and N. J. Dovichi (Eds.). (1992) Advances in DNA sequencing technology. In R. A. Keller, L. A. Bottomly and N. J. Divichi (Eds.) *Advances in DNA Sequencing Technology*. Vol. 1891, Los Angeles, S. P. I. E.
16. S. C. Hung, R. A. Mathies, and A. N. Glazer (1998) *Analyt. Biochem*. **255**(1), 32–38.
17. A. Van Orden, H. Cai, P. M. Goodwin, and R. A. Keller (1999) *Analyt. Chem*. **71**(11), 2108–2116.
18. M. Sauer, B. Angerer, K. T. Han, and C. Zander (1999) *Phys. Chem. Chemical Phys*. **1**(10), 2471–2477.
19. Q. Gao, H. M. Pang, and E. S. Yeung (1999) *Electrophoresis* **20**(7), 1518–1526.
20. S. McWhorter and S. A. Soper (2000) *Electrophoresis* **21**(7), 1267–1280.
21. A. Hanning, P. Lindberg, J. Westberg, and J. Roeraade (2000) *Analyt. Chem*. **72**(15), 3423–3430.
22. L. B. Bloom, M. R. Otto, J. M. Beechem, and M. F. Goodman (1993) *Biochemistry* **32**, 11247–11258.
23. L. B. Bloom, M. R. Otto, R. Eritja, L. J. Reha-Krantz, M. F. Goodman, and J. M. Beechem (1994) *Biochemistry* **33**, 7576–7586.
24. K. D. Raney, L. C. Sowers, D. P. Millar, and S. J. Benkovic (1994) *Proc. Natl. Acad. Sci. USA* **91**, 6644–6648.
25. A. Ujvari and C. T. Martin (1996) *Biochemistry* **35(46)**(Nov. 19), 14574–14582.
26. B. W. Allan and N. O. Reich (1996) *Biochemistry* **35**(47), 14757–14762.
27. Y. Jia, A. Kumar, and S. S. Patel (1996) *J. Biol. Chem*. **271**(48), 30451–38458.
28. M. Menger, T. Tuschl, F. Eckstein, and D. Porschke (1996) *Biochemistry* **35(47)** (Nov 26), 14710–14716.
29. J. M. Beechem, M. R. Otto, L. B. Bloom, R. Eritja, L. J. Reha-Krantz, and M. F. Goodman (1998) *Biochemistry* **37**(28), 10144–10155.
30. M. R. Otto, L. B. Bloom, M. F. Goodman, and J. M. Beechem (1998) *Biochemistry* **37**(28), 10156–10163.
31. L. J. Reha-Krantz, L. A. Marquez, E. Elisseeva, R. P. Baker, L. B. Bloom, H. B. Dunford, and M. F. Goodman (1998) *J. Biol. Chem*. **273**(36), 22969–22976.
32. W. C. Lam, E. J. Van der Schans, L. C. Sowers, and D. P. Millar (1999) *Biochemistry* **38**(9), 2661–2668.
33. B. W. Allan, N. O. Reich, and J. M. Beechem (1999) *Biochemistry* **38**(17), 5308–5314.
34. N. G. Walter, P. A. Chan, K. J. Hampel, D. P. Millar, and J. M. Burke (2001) *Biochemistry* **40**(8), 2580–2587.
35. T. J. Wilson, Z. Y. Zhao, K. Maxwell, L. Kontogiannis, and D. M. Lilley (2001) *Biochemistry* **40**(7), 2291–2302.
36. S. Sen, G. Krishnamoorthy, and B. J. Rao (2001) *FEBS Lett*. **491**(3), 289–298.
37. E. L. Rachofsky, E. Seibert, J. T. Stivers, R. Osman, and J. B. Ross (2001) *Biochemistry* **40**(4), 957–67.
38. E. L. Rachofsky, R. Osman, and J. B. Ross (2001) *Biochemistry* **40**(4), 946–956.
39. P. O. Lycksell, A. Graslund, F. Claesens, L. W. McLaughlin, U. Larsson, and R. Rigler (1987) *Nucleic Acids Res*. **15**(21), 9011–9025.
40. A. Gräslund, F. Claesens, L. W. McLaughlin, P.-O. Lycksell, U. Larsson, and R. Rigler. (1987) NMR and time-resolved fluorescence studies of a 2-aminopurine substituted Eco RI restriction site A. Ehrenberg, R. Rigler, A. Gräslund, and L. Nilsson (Eds.) In *Structure, Dynamics and Function of Biomolecules*, Berlin, Springer-Verlag, pp. 201–207.
41. T. M. Nordlund, S. Andersson, L. Nilsson, R. Rigler, A. Graslund, and L. W. McLaughlin (1989) *Biochemistry* **28**(23), 9095–9103.
42. P. G. Wu, T. M. Nordlund, B. Gildea, and L. W. McLaughlin (1990) *Biochemistry* **29**(27), 6508–6514.
43. K. Evans, D.-G. Xu, Y.-S. Kim, and T. M. Nordlund (1992) *J. Fluoresc*. **2**(4), 209–216.
44. D. Xu, K. O. Evans, and T. M. Nordlund (1994) *Biochemistry* **33**(32), 9592–9599.
45. D. P. Millar and T. E. Carver (1994) Proc. S.P.I.E. **2137**, 686–695.
46. D. P. Millar (1996) *Curr. Opin. Struct. Biol*. **6(3)**(Jun), 322–326.
47. T. J. Meade and J. F. Kayyem (1995) *Sci. News* **147**(8), 117.
48. D. B. Hall, R. E. Holmlin, and J. K. Barton (1996) *Nature* **382**(6593), 731–735.
49. B. Armitage, D. Ly, T. Koch, H. Frydenlund, H. Orum, H. G. Batz, and G. B. Schuster (1997) *Proc. Natl. Acad. Sci. USA* **94**(23), 12320–12325.
50. D. B. Hall and J. K. Barton (1997) *J. Am. Chem. Soc*. **119**, 5045–5046.
51. P. J. Dandliker, M. E. Nunez, and J. K. Barton (1998) *Biochemistry* **37**(18), 6491–502.
52. S. O. Kelley and J. K. Barton (1999) *Science* **283**(5400), 375–381.
53. C. Wan, T. Fiebig, O. Schiemann, J. K. Barton, and A. H. Zewail (2000) *Proc. Natl. Acad. Sci. USA*. **97**(26), 14052–14655.
54. M. Aida, K. Yamane, and C. Nagata (1986) *Mutation Res*. **173**(1), 49–54.
55. W. P. Diver and D. M. Woodcock (1989) *Mutagenesis* **4**(4), 302–305.
56. G. Speit, S. Garkov, S. Haupter, and B. Koberle (1990) *Mutagenesis* **5**(2), 185–190.

57. L. A. Marquez and L. J. Rehakrantz (1996) *J. Biol. Chem*. **271(46)** (Nov. 15), 28903–28911.
58. M. F. Goodman and K. D. Fygenson (1998) *Genetics* **148**(4), 1475–1482.
59. B. T. Smith, A. D. Grossman, and G. C. Walker (2001) *Mol. Cell* **8**(6), 1197–1206.
60. T. M. Nordlund, D. Xu, and K. O. Evans (1993) *Biochemistry* **32**, 12090–12095.
61. D. Xu. (1996) Sequence Dependent Energy Transfer in DNA Oligonucleotides. Ph.D. thesis, University of Alabama at Birmingham.
62. D. Xu and T. M. Nordlund (2000) *Biophys. J*. **78**(2), 1042–1058.
63. M. Kawai, M. J. Lee, K. O. Evans, and T. M. Nordlund (2001) *J. Fluoresc*. **11**(1), 23–32.
64. D. C. Ward, E. Reich, and L. Stryer (1969) *J. Biol. Chem.* **244**, 1228–1237.
65. A. Kawski, B. Bartoszewicz, I. Gryczynski, and M. Krajewski (1975) *Bull. L'Acad. Polon. Sci*. (Serie des sciences math., astr. et phys.) **XXIII**, 367–372.
66. A. Bierzynski, H. Kozlowska, and K. L. Wierzchowski (1977) *Biophys. Chem*. **6**, 223–229.
67. K. O. Evans. (1998) Dynamic characterization of 2-aminopurine in oligonucleotides using fluorescence, magnetic resonance, and Raman spectroscopies. Ph.D. thesis, University of Alabama at Birmingham.
68. T. M. Nordlund, R. Rigler, and J. Y. Chattopadhyaya. (1987). Nordlund, Rigler and Chattopadhyaya observed strong red-shifted emission from a 5′-2′-tri-ribonucleotide containing two 2-aminopurines.
69. G. Wenska (1989) *J. Photochem. Photobiol*. A **49**, 167–185.
70. J. M. Jean and K. B. Hall (2001) *Proc. Natl. Acad. Sci. USA* **98**(1), 37–41.
71. J. D. Puglisi and I. J. Tinoco. (1989) Absorbance melting curves of RNA. In J. E. Dahlberg and J. N. Abelson (Eds.) *RNA Processing, Part A General Methods*, Vol. 180, *Methods in Enzymology*, San Diego, Academic Press, pp. 304–325.
72. N. Le Novère (2001) *Bioinformatics* **17**, 1226–1227.
73. T. M. Nordlund, D. Xu, and K. O. Evans (1993) *Biochemistry* **32**(45), 12090–12095.
74. J. R. Lakowicz. (1999) *Principles of Fluorescence Spectroscopy*, 2nd ed., New York, Kluwer Academic/Plenum Publishers.
75. S. P. Davis, T. Truss, and T. M. Nordlund. (2002). Unusual energy transfer and structures in guanine oligodeoxynucleotides. In *March, 2002*, *Meeting of the American Physical Society*, **47**(1). *Bull. Amer*. Phys. Soc., pp. L32.009. American Physical Society, Indianapolis.
76. M. Gueron, J. Eisinger, and R. G. Schulman (1967) *J. Chem. Phys*. **47**(10), 4077–4091.
77. J. Eisinger, A. A. Lamola, J. W. Longworth, and W. B. Gratzer (1970) *Nature* **226**(241), 113–118.
78. M. Gueron, J. Eisinger, and A. A. Lamola. (1974) In P.O.P.T'so (Ed.) *Basic Principles in Nucleic Acid Chemistry*, Vol. I, New York, Academic Press, pp. 311–398.
79. P. Vigny and J. P. Ballini. (1977) Excited states of nucleic acids at 300K and electronic energy transfer. In B. Pullman and N. Goldblum (Eds.) *Excited States in Organic Chemistry and Biochemistry*, Dordrecht, D. Reidel Publishing Co., pp. 1–13.
80. S. Georghiou, S. Zhu, R. Weidner, C.-R. Huang, and G. Ge (1990) *J. Biomolec. Struct. Dynamics* **8**(3), 657–674.